

## THE EFFECT OF FREEZE- DRYING METHOD FOR $\beta$ -TCP NANOCRYSTALS OBTENTION

---

***Gabriel Cardoso Pinto***

São Paulo State University (Unesp),  
Laboratory of Magnetic Materials and  
Colloids (LaMMC), Physical Chemistry  
Department, Institute of Chemistry  
São Paulo State University (Unesp),  
Laboratory of Biomaterials, Physical  
Chemistry Department, Institute of  
Chemistry, Araraquara, Brazil

***Caio Carvalho dos Santos***

São Paulo State University (Unesp),  
Laboratory of Magnetic Materials and  
Colloids (LaMMC), Physical Chemistry  
Department, Institute of Chemistry,  
Araraquara, Brazil

***Rodolfo Debone Piazza***

São Paulo State University (Unesp),  
Laboratory of Magnetic Materials and  
Colloids (LaMMC), Physical Chemistry  
Department, Institute of Chemistry,  
Araraquara, Brazil

***Guilherme Nunes Lucena***

São Paulo State University (Unesp),  
Laboratory of Magnetic Materials and  
Colloids (LaMMC), Physical Chemistry  
Department, Institute of Chemistry,  
Araraquara, Brazil

***Jorge Enrique Rodriguez Chanfrau***

São Paulo State University (Unesp),  
Laboratory of Biomaterials, Physical  
Chemistry Department, Institute of  
Chemistry, Araraquara, Brazil

All content in this magazine is  
licensed under a Creative Com-  
mons Attribution License. Attri-  
bution-Non-Commercial-Non-  
Derivatives 4.0 International (CC  
BY-NC-ND 4.0).



**Antônio Carlos Guastaldi**

São Paulo State University (Unesp),  
Laboratory of Biomaterials, Physical  
Chemistry Department, Institute of  
Chemistry, Araraquara, Brazil

**Miguel Jafelicci Junior**

São Paulo State University (Unesp),  
Laboratory of Magnetic Materials and  
Colloids (LaMMC), Physical Chemistry  
Department, Institute of Chemistry,  
Araraquara, Brazil

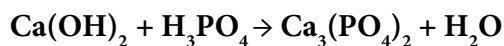
**Rodrigo Fernando Costa Marques**

São Paulo State University (Unesp),  
Laboratory of Magnetic Materials and  
Colloids (LaMMC), Physical Chemistry  
Department, Institute of Chemistry  
Monitoring and Research Center for the  
Quality of Fuels, Biofuels, Petroleum and  
Derivatives (CEMPEQC/IQ-Unesp),  
Araraquara, Brazil

**Abstract:** Calcium phosphates are the major inorganic compound found in hard human tissues, being then the main material used to mimetite bone tissues, and considering the increase in the expectation and quality of life, the development of biomaterials for tissue regeneration is of great importance and their demand increases every day. In this work, it was studied the influence of freeze-dry method for the synthesis of nanocrystals of calcium phosphates in the tricalcium phosphate ( $\beta$ -TCP) phase due to its similarity with the natural bone. This procedure affects the morphologic and crystallinity characteristics of the  $\beta$ -TCP phase. X-ray diffractograms confirmed a higher degree of crystallinity in the  $\beta$ -TCP freeze-dried. Scanning electron microscopy (SEM) histograms from the images of both samples confirmed that the freeze-dried one has presented a narrower particle size distribution with 150 nm average diameter particles, conferring it a technological advantage for bone regeneration applications to prevent the immunological adverse effects.  
**Keywords:** Tissue engineering, Calcium phosphates, biomaterial, lyophilization.

## INTRODUCTION

Included in the group of ceramic biomaterials are calcium phosphate derivatives, widely used in medical applications due to their similarity with biological apatite, found in an abundant form (about 65% to 70%) in the composition of bones and teeth [1–3]. Its synthesis occurs mainly by the reaction, in a wet chemical method, with phosphoric acid and calcium hydroxide through an acidic/basic reaction, as exemplified in Equation 1 [4,5]



Equation 1.

Calcium phosphates derivated can be differentiated and classified through their molar ratio between calcium and phosphorus (Ca/P), which can variate from 0.5 to 2.0 [6]. The composition with the highest Ca/P ratio results in a compound with low solubility in neutral conditions and a low degradation rate [7,8]. Calcium phosphates with different stoichiometries can be obtained with changed synthetic parameters such as pH, temperature, pressure, and time reactions must be considered [9].

Among the calcium phosphate derivatives most widespread in biomedical applications are hydroxyapatite, calcium phosphate cement and tricalcium phosphates [10–12]. Hydroxyapatite (HA, formula  $\text{Ca}_{10}(\text{PO}_4)_6(\text{OH})$ ) had a hexagonal crystalline system, is a biomaterial that has a unique advantage of implant/tissue adhesion, caused by its easy bone adaptation caused by its chemistry structure similarity with natural bone [13]. Due to its high insolubility (Ca/P = 1.67), its degradation in the human body occurs slowly, thus limiting its application [14]. The cements are an inorganic paste that harden due to the precipitation of one or more calcium phosphates, which can then be applied directly to the body and at room temperature. However, its disadvantage is related to the absence of micropores in its structure, thus preventing the growth of internal cells [15].

The tricalcium phosphates (TCP,  $\text{Ca}_3(\text{PO}_4)_2$ ), however also presenting four polymorphs forms, such as  $\alpha$ ,  $\beta$ ,  $\alpha'$  and  $\gamma$  [16,17]. The difference in their polymorphs will then be found in the crystalline phase, resulting in differences in protein adsorption and solubility [18].  $\beta$ -TCP is composed of a rhombohedral crystalline system, and it is among the other polymorphs, the most studied phase due to its more excellent chemical stability and the characteristic of being better absorbable by the organism and

interacting with the natural bone [19].

Due to its similarity with bone tissue, containing Ca/P = 1.5 and wettability of the surface,  $\beta$ -TCP allows nutrients to pass through its structure, thus facilitating bone growth in the desired region [20]. In addition to its wide use for filling fractures and bone cavities,  $\beta$ -TCP allows the exchange of ions  $\text{Ca}^{2+}$  and  $\text{PO}_4^{3-}$  with the physiological medium [21,22]. To further improve the characteristics of  $\beta$ -TCP, the formation of a ceramic biomaterial with high crystallinity and homogeneity of particles, allowing easy interaction with natural bone with this biomaterial is essential for its medical use to be even more widespread.

In this way, it is described in this work the influence of the freeze-drying method for the  $\beta$ -TCP synthesis and how this procedure affects the morphologic and crystallinity characteristics of the interest phase of this biomaterial.

## EXPERIMENTAL SECTION

### MATERIALS

Without any previous treatment, the following reagents were used: Calcium hydroxide ( $\text{Ca}(\text{OH})_2$ , 96.0%), and a saline phosphate buffer solution (PBS: 0.01 mol L<sup>-1</sup> phosphate, 0.135 mol L<sup>-1</sup> NaCl and 0.002 mol L<sup>-1</sup> KCl) were purchased from Sigma-Aldrich Brazil. Phosphoric acid ( $\text{H}_3\text{PO}_4$ , ACS 85.0%) was purchased from Synth Brazil.

### SYNTHESIS OF CALCIUM PHOSPHATES

Through a wet chemical method, the precursor of  $\beta$ -TCP was synthesized [23]. The calcium hydrogen phosphate dihydrate (DCPD) phase was obtained by dropwising 30 drops per minute of 200 mL phosphoric acid solution (0.6 mol L<sup>-1</sup>) over 200 mL of calcium hydroxide solution (1.0 mol L<sup>-1</sup>) under mechanical stirring (300 rpm) during

three hour. The solution with DCPD was kept in rest for 2 h, the filtration was required for the removal of the aqueous medium. Two fractions of this sample were separated, one was freeze-dried and the other was dried at room temperature. For the obtention of  $\beta$ -TCP, both DCPD powder fractions were calcinated at 800 °C for three hour.

## CHARACTERIZATION

Fourier transform infrared (FT-IR) spectra were recorded on a VERTEX 70 spectrometer from BRUKER with ATR module (Mid-infrared absorption spectroscopy by attenuated total reflection (diamond crystal)) in the spectral range of 400–4000  $\text{cm}^{-1}$ , using the resolution set at 4  $\text{cm}^{-1}$  and 64 scans. The Scanning Electron Microscopy (SEM) images and Energy Dispersive X-Ray Analysis (EDX), for morphologic, size and composition determination, were obtained by JEOL JSM 7500F microscopy and the samples were coated by C. The crystalline phases were evaluated by X-ray powder diffraction (XRD) technique. XRD were acquired using a Rigaku-Rint 2000 diffractometer with a  $\text{CuK}\alpha$  radiation source. The samples were recorded from 5 to 80° of  $2\theta$ , with a step of 0.01°. The software ImageJ (version 1.45s) was used for image treatment.

## RESULTS AND DISCUSSION

### SYNTHESIS OF FREEZE-DRIED AND NON-FREEZE DRIED $\beta$ -TCP

All the characterization of the DCPD precursor can be found in the supplementary data. To determine the best way to obtain  $\beta$ -TCP particles, a comparative study between the synthesis method using freeze-drying was carried out. The X-ray diffractogram presented in Figure 1 shows the samples of freeze-dried ( $\beta$ -TCP FD) and non-freeze dried ( $\beta$ -TCP N/FD) compared to its standard. It is observed that the main diffraction peaks present in

the  $\beta$ -TCP pattern are also present in both synthesized samples, corroborating that both calcium phosphates thus have the crystalline phase characteristic of  $\beta$ -TCP [19].

The  $\beta$ -TCP N/FD sample has in the region of 10 to 25° absence of crystalline periodicity, attributed to amorphous compounds and differences in intensity of some diffraction peaks when compared to the standard, possibly caused by the presence of other crystalline phases calcium phosphate in addition to  $\beta$ -TCP, such as the precursor DCPD. The  $\beta$ -TCP FD sample already has a much more crystalline behavior and its diffraction peaks directly coincide with the pattern.

The hypothesis raised to explain these differences is in the presence of water in the precursor DCPD used without being dried beforehand. The thermal energy used to form the  $\beta$ -TCP N/FD sample was also spent, throughout sintering, to remove all water from the system through evaporation. In contrast, for the  $\beta$ -TCP FD sample, this energy was used integrally for calcium phosphate phase change because due to the lyophilization treatment, this sample no longer had water. Thus, it is possible to conclude that the thermal energy applied in the lyophilized precursor enabled the formation of the  $\beta$ -TCP crystalline phase in a much more effective way and guaranteeing a high crystallinity index.

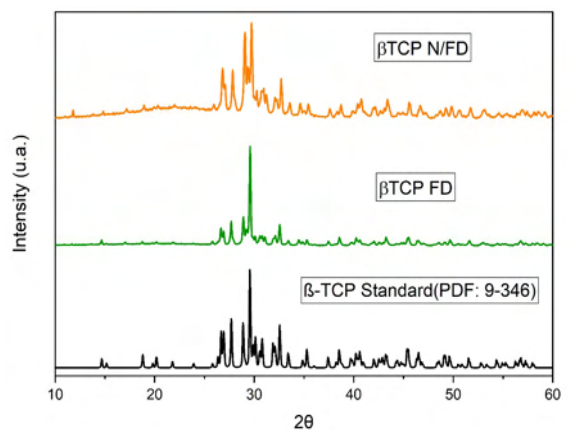


Figure 1: X-ray diffractogram comparing the  $\beta$ -TCP pattern with  $\beta$ -TCP N/FD and  $\beta$ -TCP FD samples.

To confirm once again the presence of the main functional groups present in compounds derived from calcium phosphates, the infrared spectroscopy technique was used (Figure 2). The  $\beta$ -TCP N/FD and  $\beta$ -TCP FD samples do not have water-related bands, due to the sintering process occurring at 800 °C. Infrared absorption bands at 500, 550, 900 and 970  $\text{cm}^{-1}$ , found in the two samples, can be attributed to the  $\text{PO}_4^{3-}$  ions [23]; the 1000 to 1200  $\text{cm}^{-1}$  region is related to the P = O bond; the last band found in both samples is the one found at 715  $\text{cm}^{-1}$ , characteristic of the P-O-P symmetrical mode [24]. All identified bands confirm the presence of the main functional groups present in  $\beta$ -TCP.

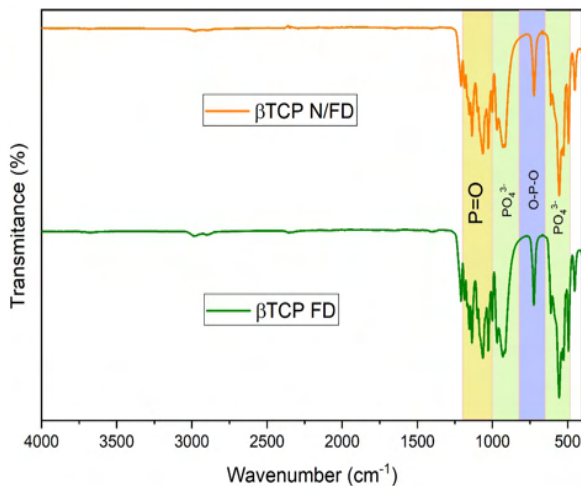


Figure 2: Spectra in the Infrared region of the  $\beta$ -TCP N/FD and  $\beta$ -TCP FD samples.

Through the thermogravimetric analysis it was possible to determine the thermal behavior of the  $\beta$ -TCP N/FD and  $\beta$ -TCP FD samples, as shown in Figure 3. For the  $\beta$ -TCP FD sample, the minimum mass loss is found, about 0.7% of the initial mass, due to the presence of free water adsorbed on the surface of the compost. The  $\beta$ -TCP N/FD sample, on the other hand, showed a loss of 1.9% of the initial mass, also associated with free water on the surface, as well as being the result of other residual crystalline phases of calcium

phosphates being converted into  $\beta$ -TCP [25].

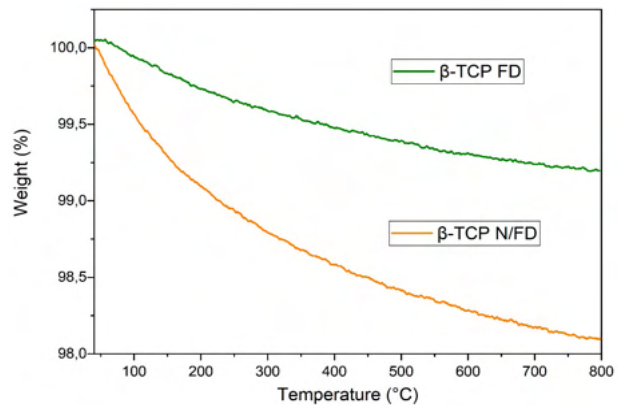


Figure 3: Thermogravimetric curve of the  $\beta$ -TCP N/FD and  $\beta$ -TCP FD samples.

SEM microscopy was used to determine the morphology of  $\beta$ -TCP N/FD and  $\beta$ -TCP FD samples. In Figure 4 (A and B) the size of the nanoparticles of  $\beta$ -TCP N/FD and  $\beta$ -TCP FD samples was compared. After the heat treatment it is possible to observe the following characteristics in the two samples: the formation of spherical (or globular) nanoparticles and massive growth of particles, causing a densification of the compound, as already reported in the literature [24].

Figure 4 shows the samples' micrograph, where it is possible to observe (both samples Figure 4 A and C) the grain with morphology roughly formed by aggregates of spheres coalesced due to sintering of the material. The histograms (Figure 4 B and D) show an average size of  $151 \pm 27$  nm and  $157 \text{ nm} \pm 17$  nm for the  $\beta$ -TCP N / FD and  $\beta$ -TCP N / FD samples, respectively, indicating a minor difference in the freeze-drying influence in the average grain size. Based on the mean and standard deviation, the polydispersity index of the grains was calculated, given by the square of the ratio of the standard deviation to the average size, the PDI values obtained were 0.032 and 0.012, respectively indicating that the two materials obtained are monodisperse [26]. It clear that the FD process in the nanomaterial

directly influences the distribution of the grains and that the lyophilization of the material allowed the formation of material with more homogeneous sizes. Considering that the application of these compounds will be directed to bone substitution, the homogeneity and high degree of purity of the biomaterial is fundamental to prevent the occurrence of infections, inflammations, and adverse allergic reactions in the patient's body.

The qualitative analysis of the main elements presents in the samples of  $\beta$ -TCP N/FD and  $\beta$ -TCP FD samples was carried out again using X-ray energy dispersive spectroscopy (EDX), Figure 5 (A and B). The presence of oxygen, calcium, phosphorus was

again observed, being yet another indication of the presence of the  $\beta$ -TCP phase in samples derived from DCPD.

## CONCLUSION

Using the wet chemical method already reported in the literature, it was possible to successfully synthesize the precursor DCPD. The use of the pre-treatment of freeze-drying of DCPD by lyophilization proved to be effective so that the synthesized  $\beta$ -TCP had homogeneity and high crystallinity in its calcium phosphate particles. The freeze-drying process ensured that the particles obtained a smaller average size, compared to the non-freeze-dried samples. Thus, the pre-

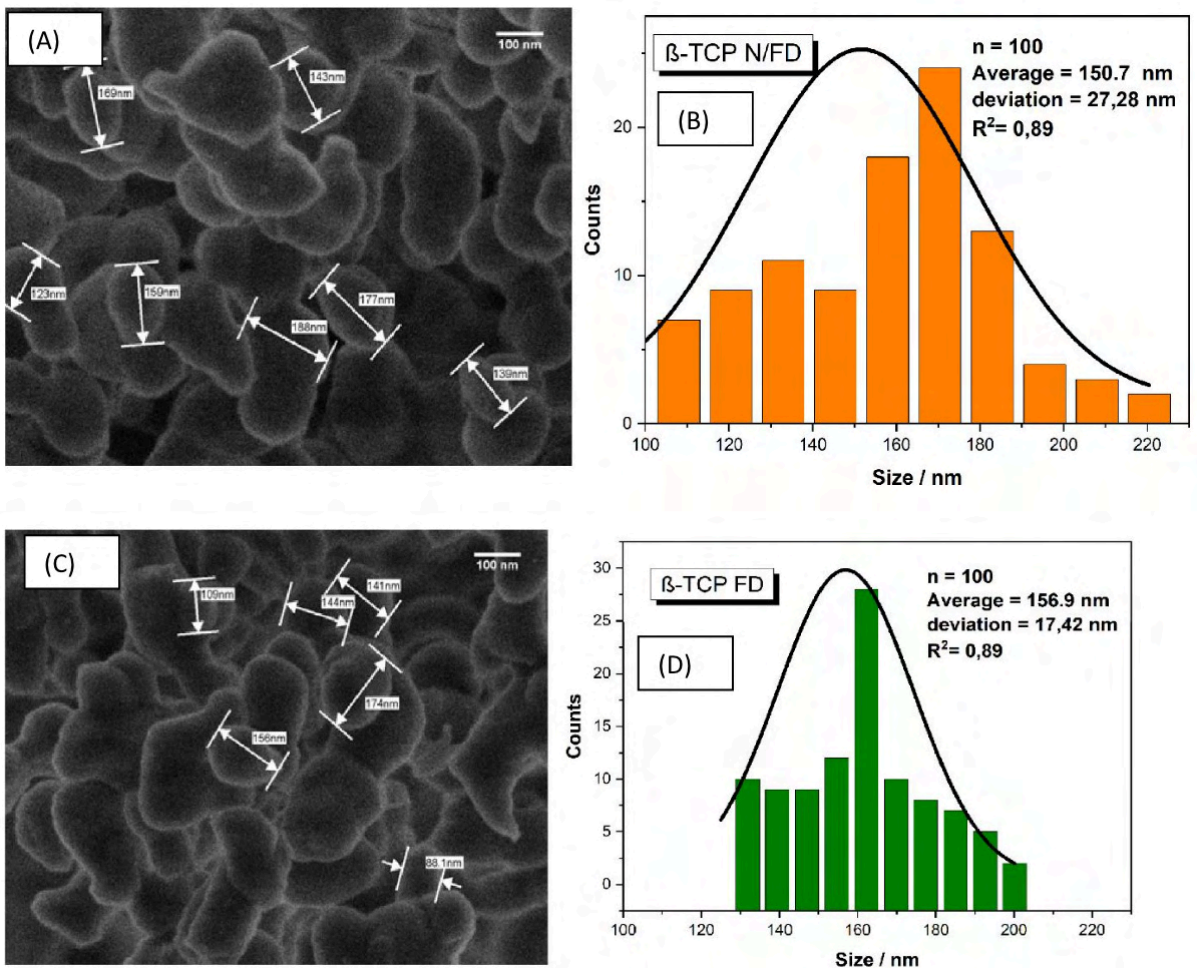


Figure 4: SEM and nanoparticle size distribution chart of the (A)  $\beta$ -TCP N/FD and (B)  $\beta$ -TCP FD samples.

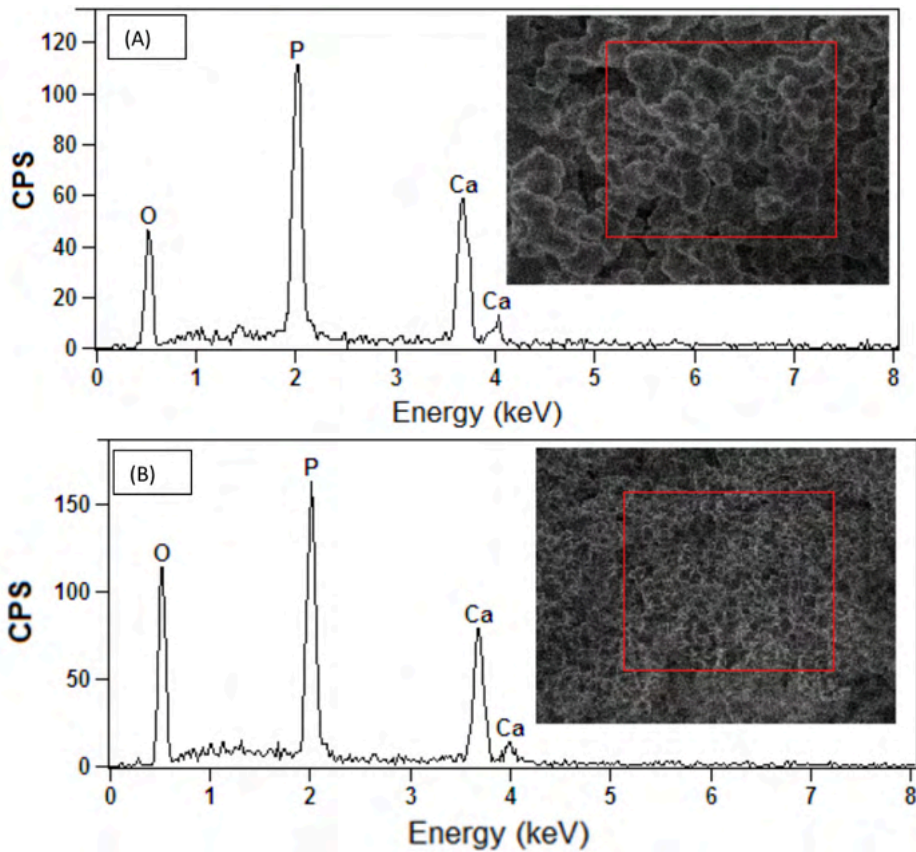


Figure 5: EDX of the (A)  $\beta$ -TCP N/FD and (B)  $\beta$ -TCP FD samples.

treatment of freeze-drying confirmed to be an adequate and simple technique to obtain nanocrystalline calcium phosphates for bone regeneration applications.

## ACKNOWLEDGEMENTS

The authors are grateful for the financial support provided by the Brazilian funding agencies FAPESP, CNPq and Finep.

## REFERENCES

1. N. Eliaz, N. Metoki, Calcium phosphate bioceramics: A review of their history, structure, properties, coating technologies and biomedical applications, *Materials*. 10 (2017). doi:10.3390/ma10040334.
2. K.M.Z. Hossain, U. Patel, A.R. Kennedy, L. Macri-Pellizzeri, V. Sottile, D.M. Grant, B.E. Scammell, I. Ahmed, Porous calcium phosphate glass microspheres for orthobiologic applications, *Acta Biomaterialia*. 72 (2018) 396–406. doi:10.1016/j.actbio.2018.03.040.
3. M. Losada, R. González, À.P. Garcia, A. Santos, J. Nart, Treatment of Non-Contained Infrabony Defects With Enamel Matrix Derivative Alone or in Combination With Biphasic Calcium Phosphate Bone Graft: A 12-Month Randomized Controlled Clinical Trial, *Journal of Periodontology*. 88 (2017) 426–435. doi:10.1902/jop.2016.160459.
4. M. Sokolova, A. Putnins, I. Kreicbergs, J. Locs, Scale-up of wet precipitation calcium phosphate synthesis, *Key Engineering Materials*. 604 (2014) 216–219. doi:10.4028/www.scientific.net/KEM.604.216.
5. K. Salma, L. Berzina-Cimdina, N. Borodajenko, Calcium phosphate bioceramics prepared from wet chemically precipitated powders, *Processing and Application of Ceramics*. 4 (2010) 45–51. doi:10.2298/pac1001045s.
6. S. Raynaud, E. Champion, J.P. Lafon, D. Bernache-Assollant, Calcium phosphate apatites with variable Ca/P atomic ratio III. Mechanical properties and degradation in solution of hot pressed ceramics, *Biomaterials*. 23 (2002) 1081–1089. doi:10.1016/S0142-9612(01)00220-4.
7. S. Raynaud, E. Champion, P. Thomas, Calcium phosphate apatites with variable Ca/P atomic ratio I. Synthesis, characterisation and thermal stability of powders, *Biomaterials*. 23 (2002) 1065–1072.
8. S. Raynaud, E. Champion, D. Bernache-Assollant, Calcium phosphate apatites with variable Ca/P atomic ratio II. Calcination and sintering, *Biomaterials*. 23 (2002) 1073–1080. doi:10.1016/S0142-9612(01)00219-8.
9. M. Bohner, B.L.G. Santoni, N. Döbelin,  $\beta$ -tricalcium phosphate for bone substitution: Synthesis and properties, *Acta Biomaterialia*. 113 (2020) 23–41. doi:10.1016/j.actbio.2020.06.022.
10. S. V Dorozhkin, Calcium orthophosphate (CaPO<sub>4</sub>)-based bone-graft substitutes and the special roles of octacalcium phosphate materials, LTD, 2020. doi:10.1016/B978-0-08-102511-6.00011-X.
11. M. Francesca, D. Filippo, L.S. Dolci, B. Albertini, N. Passerini, P. Torricelli, A. Parrilli, M. Fini, F. Bonvicini, A. Gentilomi, S. Panzavolta, A. Bigi, A radiopaque calcium phosphate bone cement with long-lasting antibacterial effect: From paste to injectable formulation, *Ceramics International*. (2020). doi:10.1016/j.ceramint.2019.12.272.
12. G.D. Webler, Síntese e Caracterização de Cerâmicas Bifásicas de Fosfato de Cálcio (Hap/B-TCP) Puras e Dopadas com Magnésio, 2015.
13. G. de SOUZA, F. Vieira ELIAS, R. de SOUZA, F. Letícia de Souza JOAQUIM, Hidroxiapatita Como Biomaterial Utilizado Em Enxerto Ósseo Na Implantodontia: Uma Reflexão Hydroxyapatite As a Biomaterial Used in Bone Graft in Implantology: a Reflection, *Revista Odontológica de Araçatuba*. 37 (2016) 33–39. <http://apcdaracatuba.com.br/revista/2016/12/5.pdf>.
14. A. Carlos, A. Herrera, D. De Físico-química, I. De Química, U.E. Paulista, R. Prof, F. Degni, FOSFATOS DE CÁLCIO DE INTERESSE BIOLÓGICO: IMPORTÂNCIA COMO BIOMATERIAIS, PROPRIEDADES E MÉTODOS DE OBTENÇÃO DE RECOBRIMENTOS, *Quimica Nova*. 33 (2010) 1352–1358.
15. A.C.K.B. e Â.M.M. Ana Luiza R. Pires, BIOMATERIAIS: TIPOS, APLICAÇÕES E MERCADO, *Quimica Nova*. 38 (2015) 957–971.
16. I. Moreno-Gomez, Degradation of Bioresorbable Composites: Calcium Carbonate Case Studies, in: *A Phenomenological Mathematical Modelling Framework for the Degradation of Bioresorbable Composites*, 2019: p. 245–266. doi:10.1007/978-3-030-04990-4\_7.
17. R.B. Heimann, Structure, properties, and biomedical performance of osteoconductive bioceramic coatings, *Surface and Coatings Technology*. 233 (2013) 27–38. doi:10.1016/j.surfcoat.2012.11.013.

18. G. Grandi, C. Heitz, L. Alberto, M. Luciano, M. Sant, A. Filho, R. Miranda, D. Nascimento, Comparative Histomorphometric Analysis Between  $\alpha$ -Tcp Cement and  $\beta$  -Tcp/Ha Granules in the Bone Repair of Rat Calvaria, *Materials Research*. 14 (2011) 11–16. doi:10.1590/S1516-14392011005000020.
19. R.G. Carrodeguas, S. De Aza,  $\alpha$ -Tricalcium phosphate: Synthesis, properties and biomedical applications, *Acta Biomaterialia*. 7 (2011) 3536–3546. doi:10.1016/j.actbio.2011.06.019.
20. B. Yuan, Z. Wang, Y. Zhao, Y. Tang, S. Zhou, Y. Sun, X. Chen, In Vitro and In Vivo Study of a Novel Nanoscale Demineralized Bone Matrix Coated PCL/ $\beta$ -TCP Scaffold for Bone Regeneration, *Macromolecular Bioscience*. 2000336 (2020) 1–11. doi:10.1002/mabi.202000336.
21. P. Feng, P. Wu, C. Gao, Y. Yang, W. Guo, W. Yang, C. Shuai, A Multimaterial Scaffold With Tunable Properties: Toward Bone Tissue Repair, *Advanced Science*. 5 (2018) 1–15. doi:10.1002/advs.201700817.
22. J.M. Sadowska, J. Guillem-Marti, M. Espanol, C. Stähli, N. Döbelin, M.P. Ginebra, In vitro response of mesenchymal stem cells to biomimetic hydroxyapatite substrates: A new strategy to assess the effect of ion exchange, *Acta Biomaterialia*. 76 (2018) 319–332. doi:10.1016/j.actbio.2018.06.025.
23. R. Debone, T.A.G. Pelizaro, J.E. Rodriguez-chanfrau, A. Almirall, L. Serna, Y. Veranes-pantoja, Calcium phosphates nanoparticles : The effect of freeze-drying on particle size reduction, *Materials Chemistry and Physics*. 239 (2020). doi:10.1016/j.matchemphys.2019.122004.
24. S.A. Silva, R. Emilio, F. Quevedo, Citotoxicidade in vitro de nanopartículas de fosfato tricálcico-  $\beta$  sintetizado via reação em estado sólido, *Revista Matéria*. 24 (2019) 12.
25. S. Kwon, Y. Jun, S. Hong, H. Kim, Synthesis and dissolution behavior of  $\beta$ -TCP and HA /  $\beta$ -TCP composite powders, *Journal of the European Ceramic Society*. 23 (2003) 1039–1045.
26. C.C. dos Santos, W.R. Viali, E.S.N. Viali, R.F.C. Marques, M. Jafelicci Junior, Colloidal stability study of Fe<sub>3</sub>O<sub>4</sub>-based nanofluids in water and ethylene glycol, *Journal of Thermal Analysis and Calorimetry*. (2020). doi:10.1007/s10973-020-10062-w.